Supporting information

Single-molecule MicroRNA Electrochemiluminescence Detection Using Cyclometalated Dinuclear Ir(III) Complex with Synergistic Effect

Tai-Bao Gao,[a§] Jing-Jing Zhang,[b,d§] Jing Wen,[c,e§] Xue-Xiao Yang,[a] Hai-bo Ma,[c] Deng-Ke Cao*[a] and Dechen Jiang*[b]

[a]State Key Laboratory of Coordination Chemistry, School of Chemistry and Chemical Engineering, Nanjing University, Nanjing 210093, P. R. China

[b]State Key Laboratory of Analytical Chemistry for Life Science, School of Chemistry and Chemical Engineering, Nanjing University, Nanjing 210093, P. R. China

[c]Key Laboratory of Mesoscopic Chemistry of MOE, School of Chemistry and Chemical Engineering, Nanjing University, Nanjing 210093, P. R. China

[d]School of Pharmacy and Key Laboratory of Targeted Intervention of Cardiovascular Disease, Collaborative Innovation Center for Cardiovascular Disease Translational Medicine, Nanjing Medical University, Nanjing, 211126, China.

[e]School of Materials Science and Engineering, Wuhan Instituent of Technology, Wuhan 430205, P. R. China

*Corresponding author E-mail: dkcao@nju.edu.cn (Deng-Ke Cao); dechenjiang@nju.edu.cn (Dechen Jiang).

ORCID: Deng-Ke Cao, 0000-0002-8256-5413; Dechen Jiang, 0000-0002-2845-3621.

[§]These authors contributed equally.

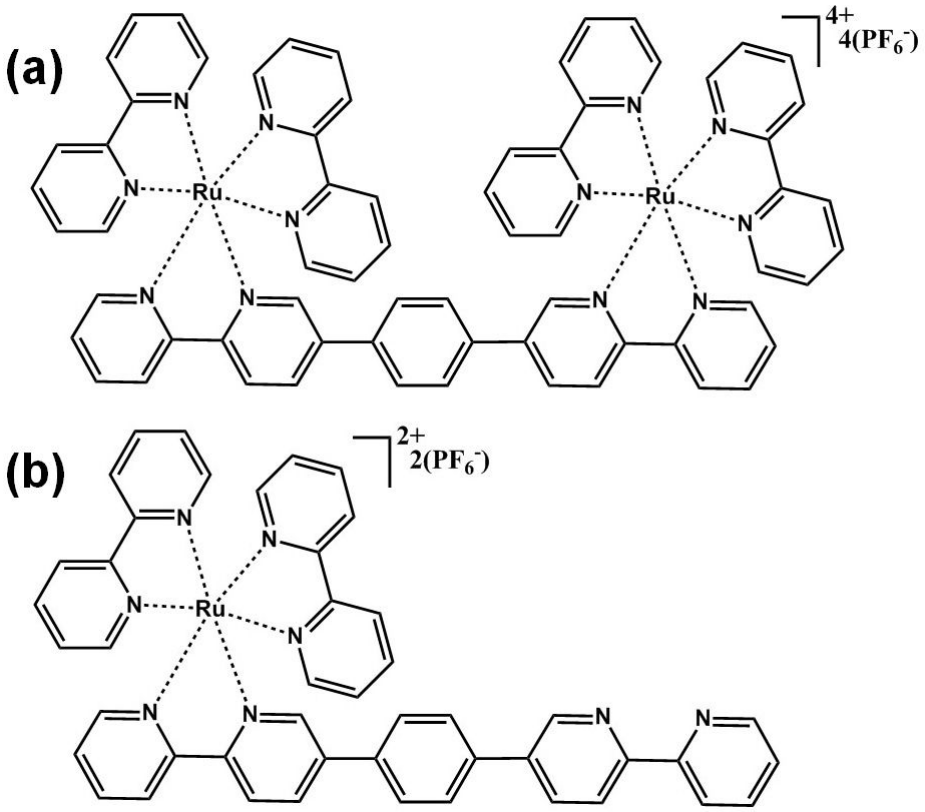

Scheme S1 The molecular structures of $\{[(bpy)_2Ru]_2(bphb)\}(PF_6)_4$ (a) and $[(bpy)_2Ru(bphb)](PF_6)_2$ (b).

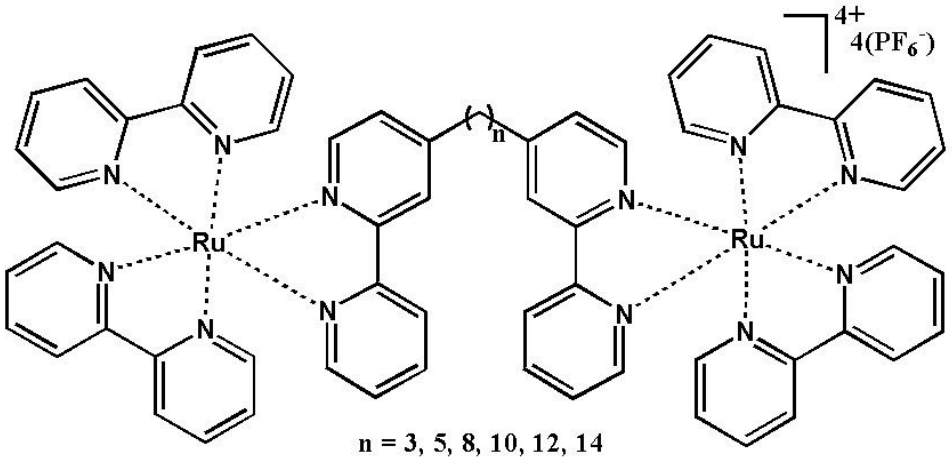

Scheme S2 The molecular structures of $[(bpy)_2Ru(bpy)(CH_2)_n(bpy)Ru(bpy)_2](PF_6)_4$.

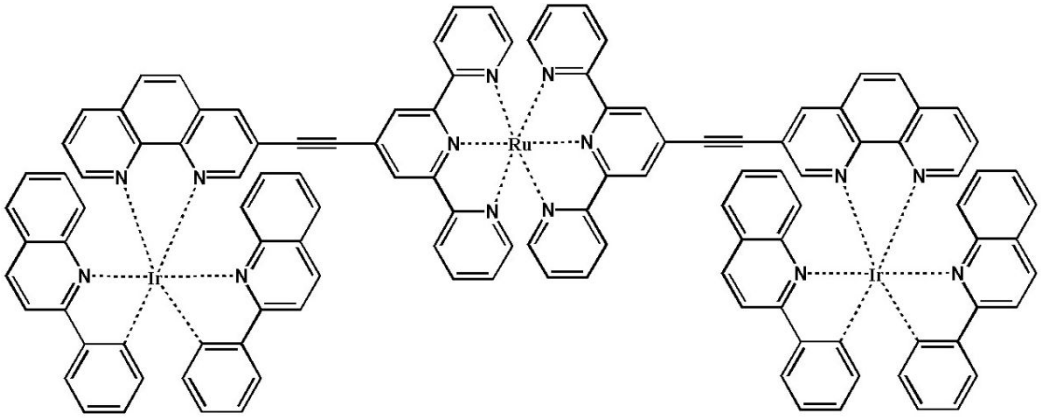

Scheme S3 The molecular structure of complex Ir(III)-Ru(II)-Ir(III).

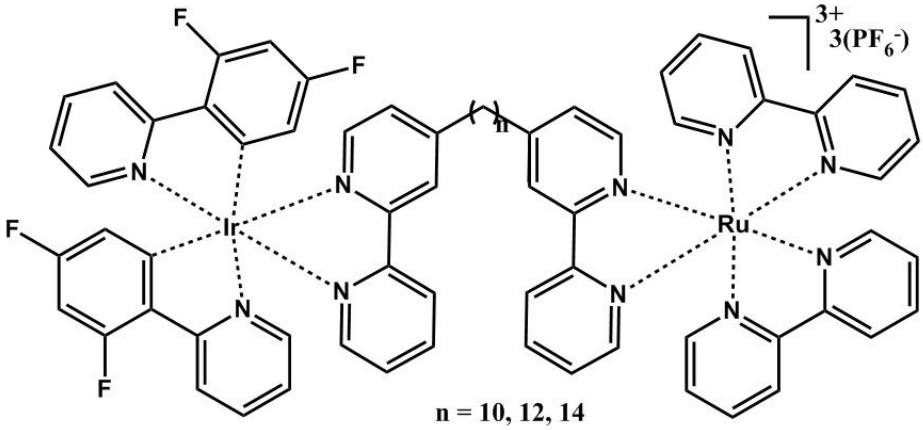

Scheme S4 The molecular structures of $[(bpy)_2Ru(bpy)(CH_2)_n(bpy)Ir(dfppy)_2](PF_6)_3$.

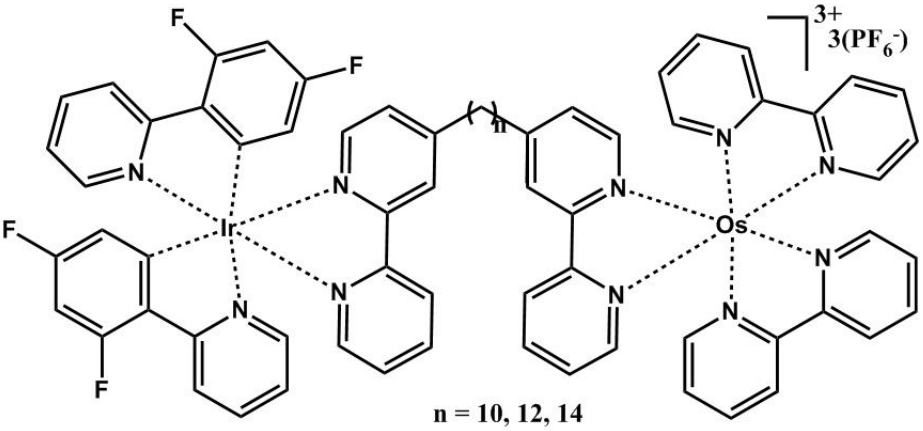

Scheme S5 The molecular structures of $[(bpy)_2Os(bpy)(CH_2)_n(bpy)Ir(dfppy)_2](PF_6)_3$.

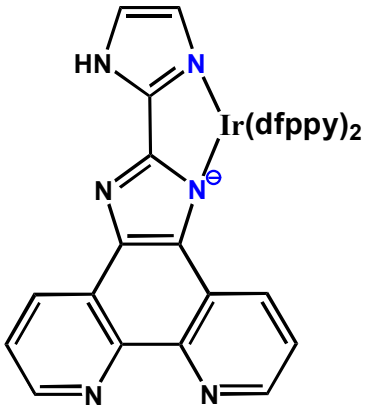

Scheme S6 The N^N$^-$ coordination mode of imiphenH$^-$ ligand in **1**·PF_6 and **2**.

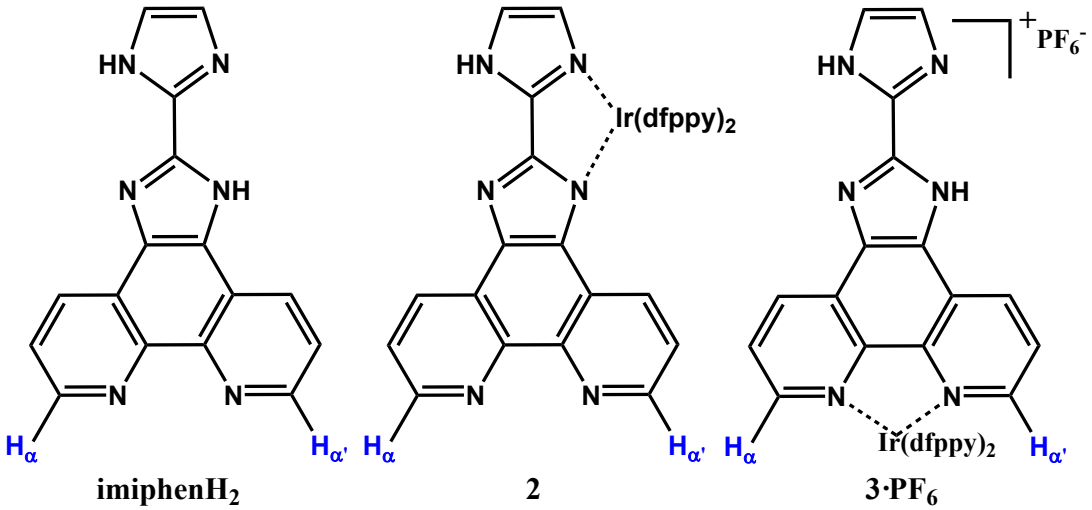

Scheme S7 The H_α and $H_{\alpha'}$ atoms in compounds imiphenH_2, **2** and **3**·PF_6.

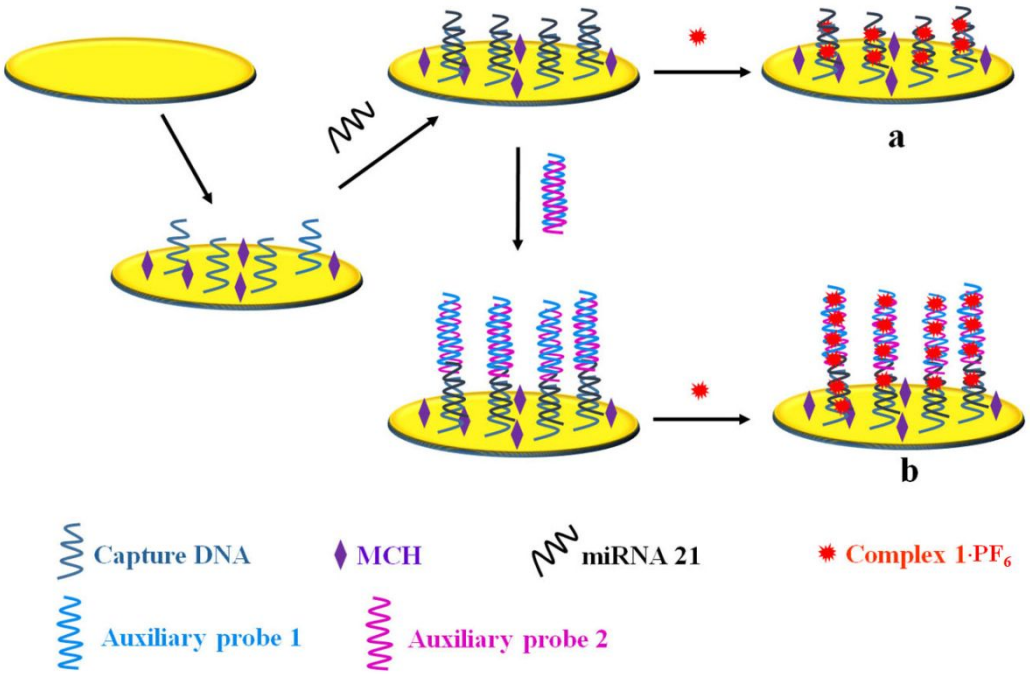

Scheme S8 Schematic diagram for the intercalation of complex **1**·PF_6 in long-range double-stranded helix and the resultant ECL detection of microRNA 21. (a: without the auxiliary probes; b: with the auxiliary probes)

Table S1 Crystallographic data and refinement for **1**·0.5PF_6·0.5OH·CH_3OH·3H_2O and **2**·H_2O.

	1·0.5PF_6·0.5OH·CH_3OH·3H_2O	**2**·H_2O
Formula	$C_{122}H_{87}N_{20}O_9F_{22}PIr_4$	$C_{38}H_{23}N_8OF_4Ir$
M	3194.88	875.84
Crystal system	Triclinic	Monoclinic
Space group	$P\bar{1}$	$P2_1/c$
T /K	296(2)	296(2)
a /Å	12.768(4)	10.273(2)
b /Å	15.562(5)	10.772(2)
c /Å	16.092(4)	29.566(6)
α /°	66.535(6)	
β /°	81.889(5)	96.413(7)
γ /°	74.185(6)	
V/Å^3	2820.0(14)	3251.4(11)
Z	1	4
D_c /g cm^{-3}	1.881	1.789
F(000)	1552	1712
GooF on F^2	1.000	1.013
R_1, wR_2 [$I>2\sigma(I)$][a]	0.0543, 0.1152	0.0599, 0.1314
R_1, wR_2 (all data)[a]	0.1036, 0.1272	0.0964, 0.1457
$(\Delta\rho)_{max}$ and $(\Delta\rho)_{min}$ (eÅ^{-3})	2.423, -1.292	0.995, -1.621

[a] $R_1 = \Sigma||F_o|-|F_c||/\Sigma|F_o|$. $wR_2=[\Sigma w(F_o^2-F_c^2)^2/\Sigma w(F_o^2)^2]^{1/2}$.

Table S2 Selected bond lengths (Å) and angles (°) for **1**·0.5PF_6·0.5OH·CH_3OH·3H_2O.

Ir1-C1	2.019(11)	Ir2-N7	2.130(8)
Ir1-C12	2.016(11)	Ir2-N8	2.119(8)
Ir1-N1	2.036(7)	Ir2-N9	2.045(7)
Ir1-N2	2.041(7)	Ir2-N10	2.032(8)
Ir1-N3	2.110(9)	N5-C26	1.363(11)
Ir1-N5	2.199(8)	N6-C26	1.337(12)
Ir2-C39	1.997(10)	N3-C25	1.337(14)
Ir2-C50	1.988(12)	N4-C25	1.359(11)
C12-Ir1-C1	88.9(4)	C50-Ir2-C39	89.3(4)
C12-Ir1-N1	97.5(4)	C50-Ir2-N10	80.1(4)
C1-Ir1-N1	80.4(3)	C39-Ir2-N10	92.1(4)
C12-Ir1-N2	80.6(4)	C50-Ir2-N9	94.6(4)
C1-Ir1-N2	93.4(3)	C39-Ir2-N9	80.7(3)
N1-Ir1-N2	173.5(4)	N10-Ir2-N9	171.2(3)
C12-Ir1-N3	92.7(4)	C50-Ir2-N8	176.4(4)
C1-Ir1-N3	172.6(3)	C39-Ir2-N8	94.2(4)
N1-Ir1-N3	92.3(3)	N10-Ir2-N8	98.6(3)
N2-Ir1-N3	94.0(3)	N9-Ir2-N8	87.1(3)
C12-Ir1-N5	168.4(3)	C50-Ir2-N7	98.7(4)
C1-Ir1-N5	102.3(3)	C39-Ir2-N7	171.0(4)
N1-Ir1-N5	87.2(3)	N10-Ir2-N7	93.4(3)
N2-Ir1-N5	95.8(3)	N9-Ir2-N7	94.4(3)
N3-Ir1-N5	76.6(3)	N8-Ir2-N7	78.0(3)

Table S3 Selected bond lengths (Å) and angles (°) for **2**·H_2O.

Ir1-C1	2.008(10)	Ir1-N5	2.229(7)
Ir1-C12	1.986(9)	N3-C25	1.346(11)
Ir1-N1	2.034(8)	N4-C25	1.355(10)
Ir1-N2	2.034(8)	N5-C26	1.364(12)
Ir1-N3	2.123(8)	N6-C26	1.329(11)
C12-Ir1-C1	86.8(4)	N2-Ir1-N3	84.9(3)
C12-Ir1-N2	80.5(3)	N1-Ir1-N3	96.8(3)
C1-Ir1-N2	98.1(4)	C12-Ir1-N5	170.6(4)
C12-Ir1-N1	97.7(4)	C1-Ir1-N5	102.4(3)
C1-Ir1-N1	80.3(4)	N2-Ir1-N5	95.9(3)
N2-Ir1-N1	177.6(3)	N1-Ir1-N5	86.2(3)
C12-Ir1-N3	93.7(3)	N3-Ir1-N5	77.2(3)
C1-Ir1-N3	177.1(4)		

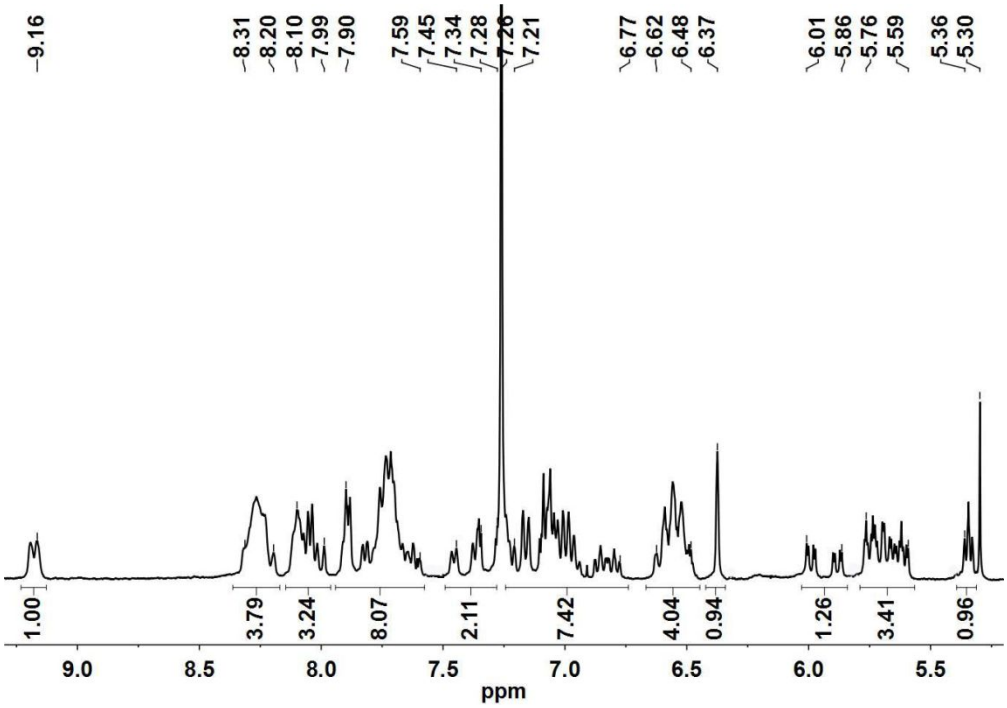

Figure S1 ^{1}H NMR spectrum of **1**·PF_6 (400 MHz, $CDCl_3$).

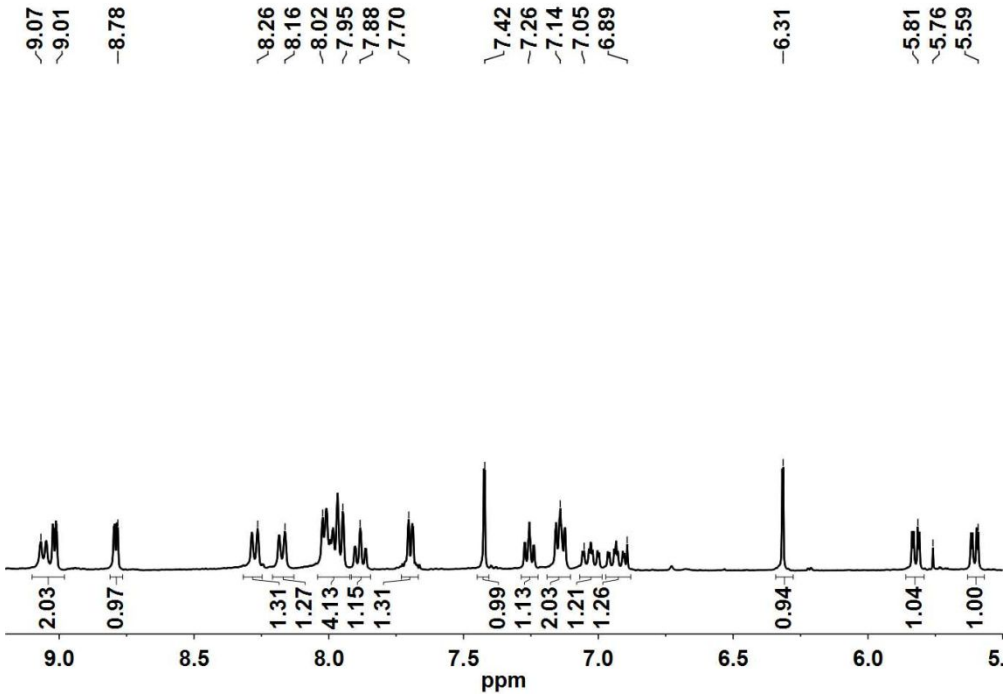

Figure S2 ^{1}H NMR spectrum of **2** (400 MHz, DMSO-d_6). The signal at 5.76 ppm is from CH_2Cl_2.

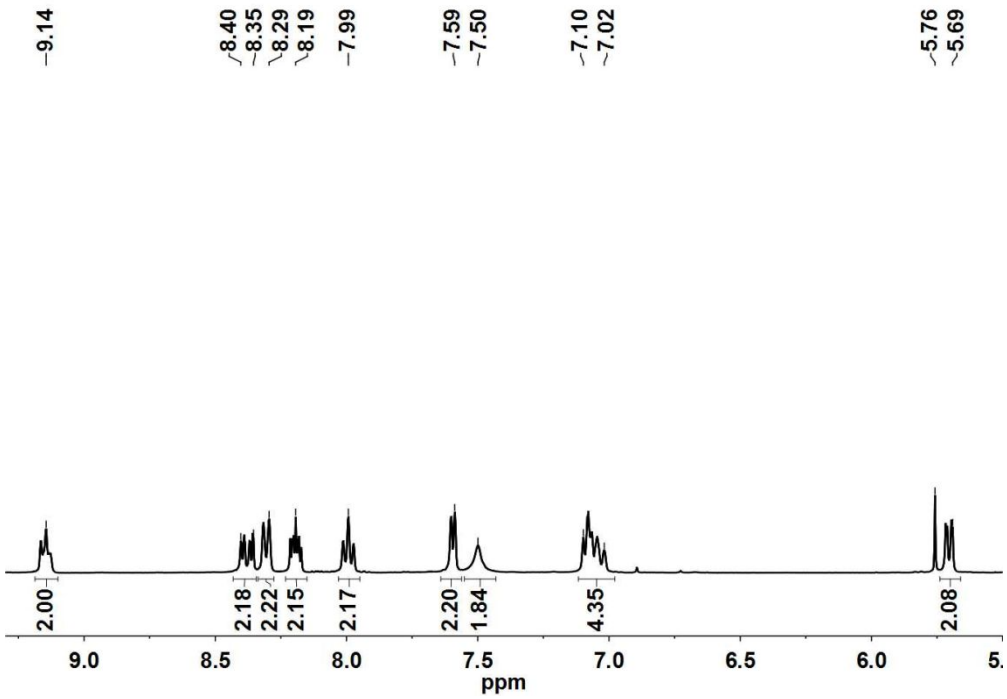

Figure S3 ^{1}H NMR spectrum of **3**·PF_6 (400 MHz, DMSO-d_6). The signal at 5.76 ppm is from CH_2Cl_2.

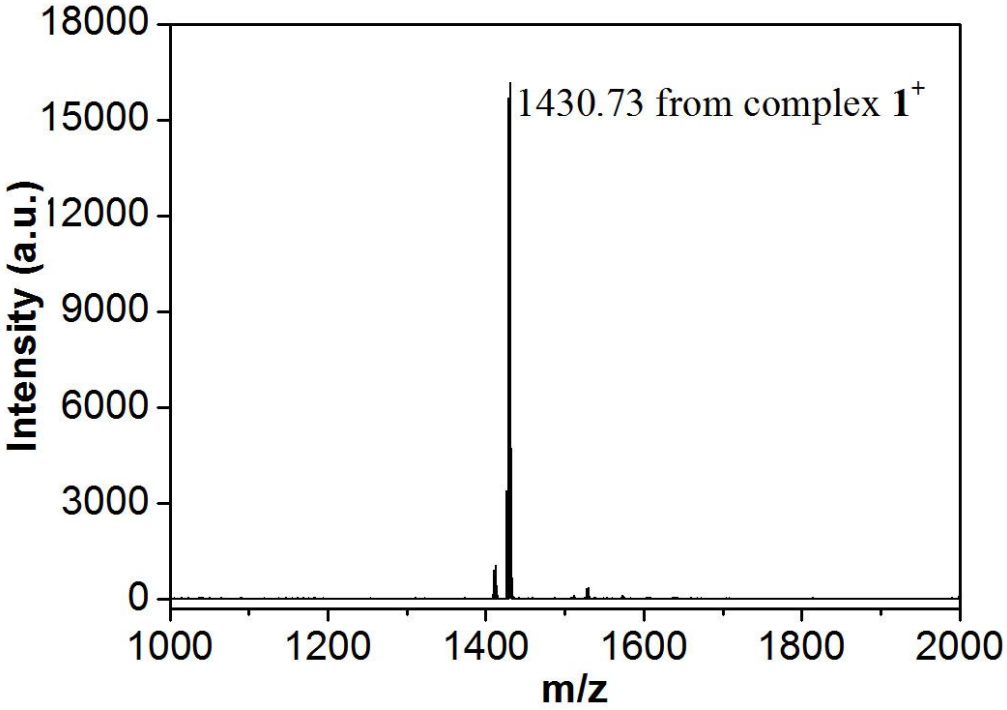

Figure S4 MALDI-TOF spectrum of **1**·PF_6.

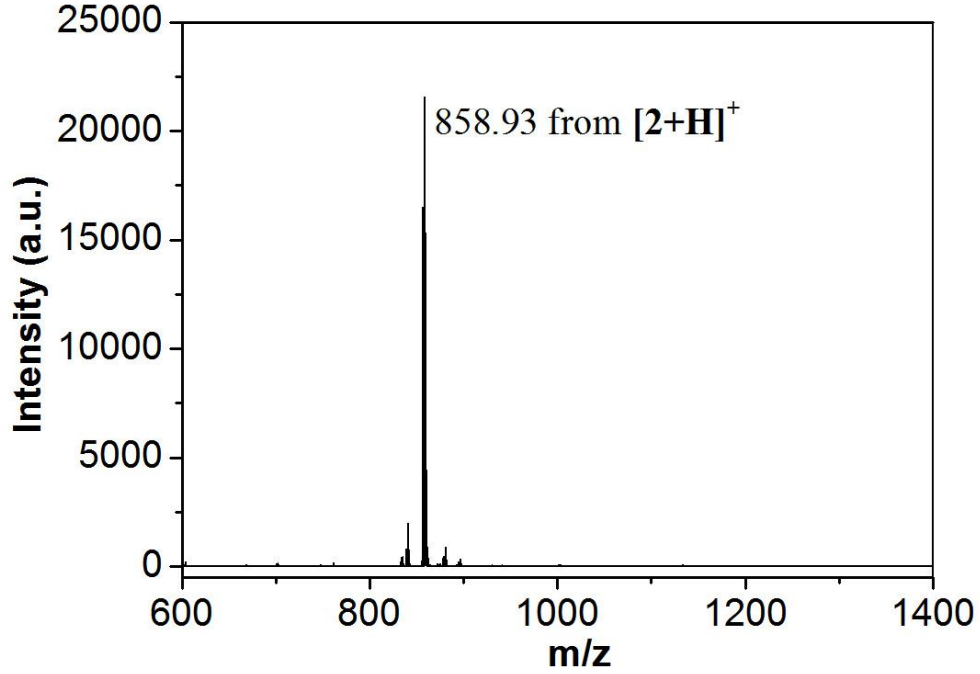

Figure S5 MALDI-TOF spectrum of **2**.

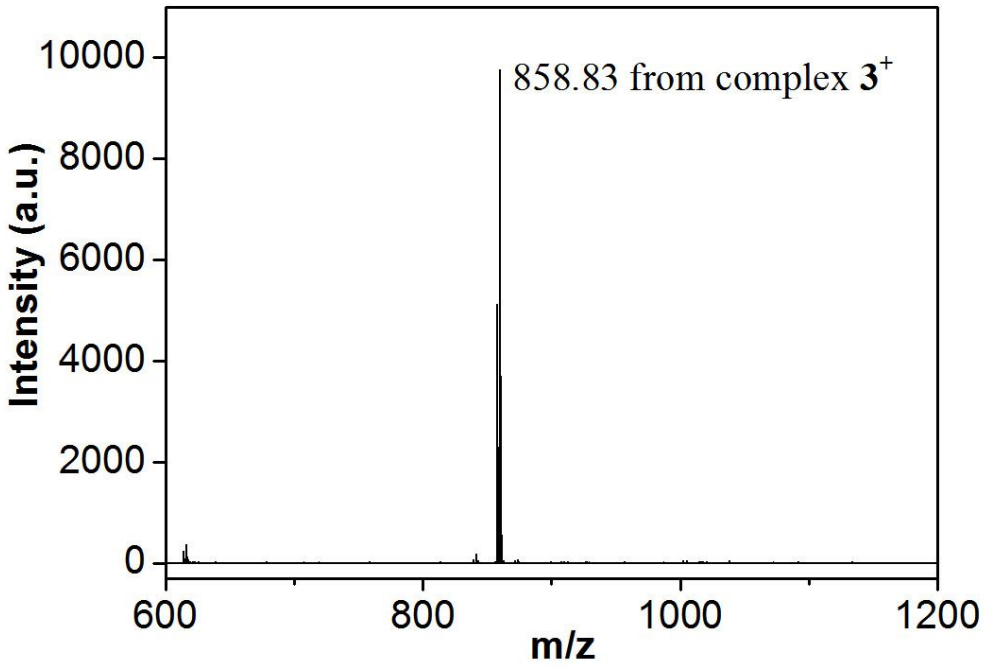

Figure S6 MALDI-TOF spectrum of **3**·PF_6.

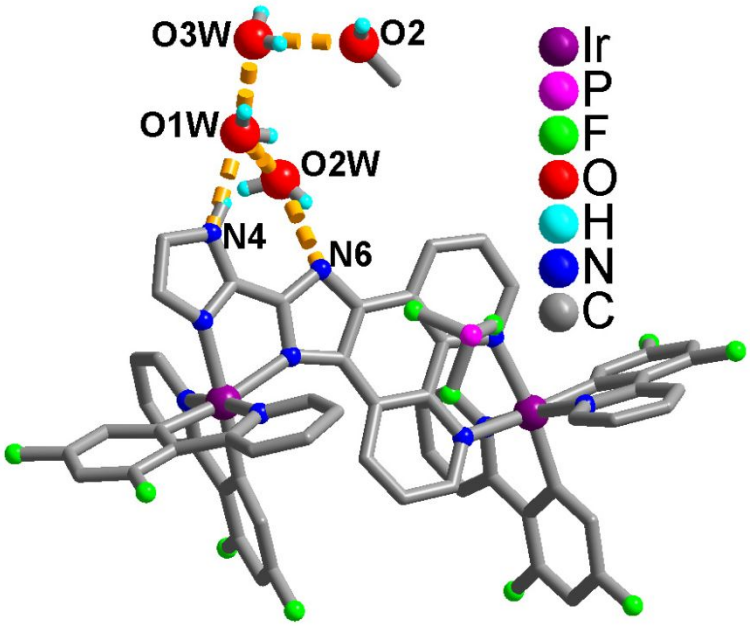

Figure S7 The hydrogen-bond connection among $[Ir_2(dfppy)_4(ImiphenH)]^+$ cation, lattice water molecules and CH_3OH molecule in **1**·0.5PF_6·0.5OH·CH_3OH·3H_2O [hydrogen bonds: O1W···O2W=2.514(1) Å, O1W···O3W=2.769 Å, O2W···N6=2.977(1) Å, N4···O1W=2.751(1) Å, and O3W···O2^a=2.718(1) Å (symmetry code a = x, y, z-1)].

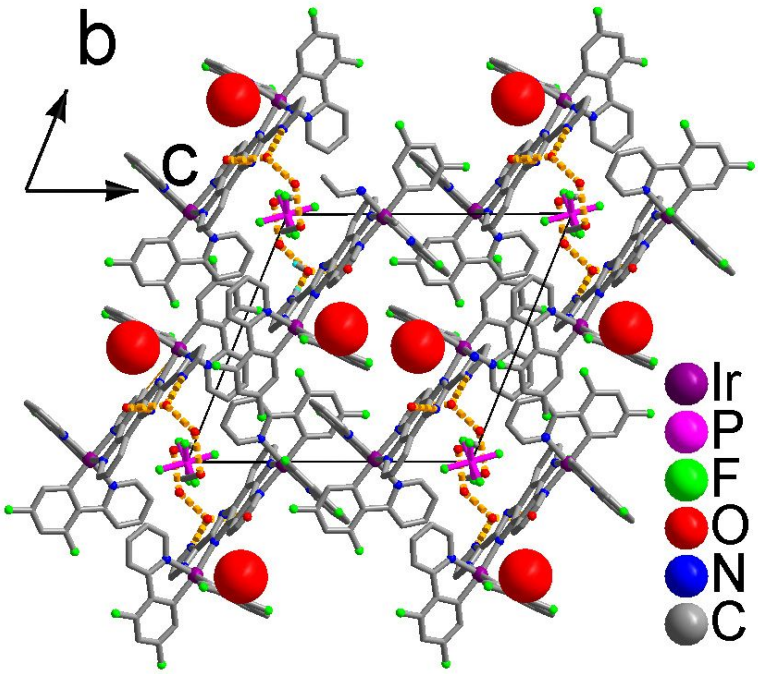

Figure S8 The packing structure of **1**·0.5PF_6·0.5OH·CH_3OH·3H_2O. Small red balls are O atoms from lattice water molecules and CH_3OH molecules, and big red balls are O atoms from OH^-.

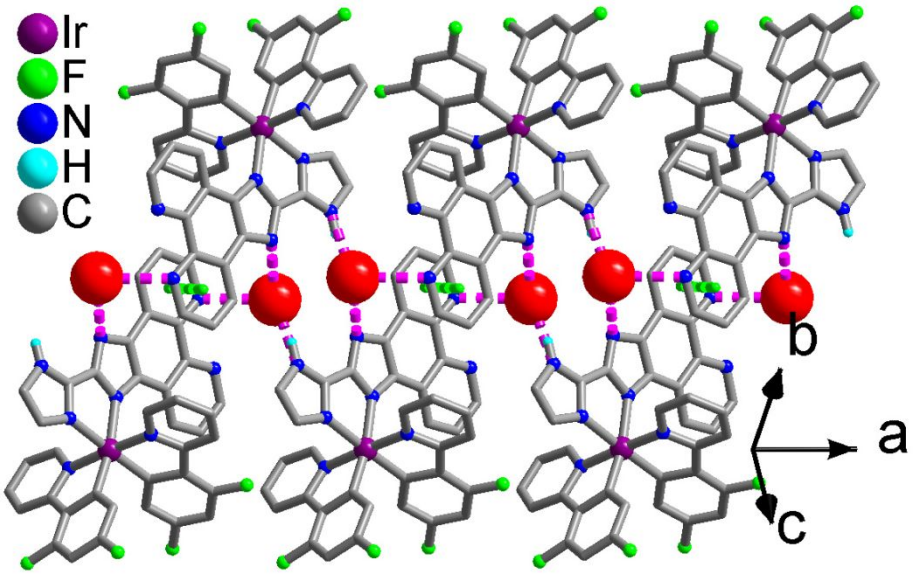

Figure S9 The supramolecular chain structure in complex **2**·H_2O. Big red balls are O atoms from lattice water molecules.

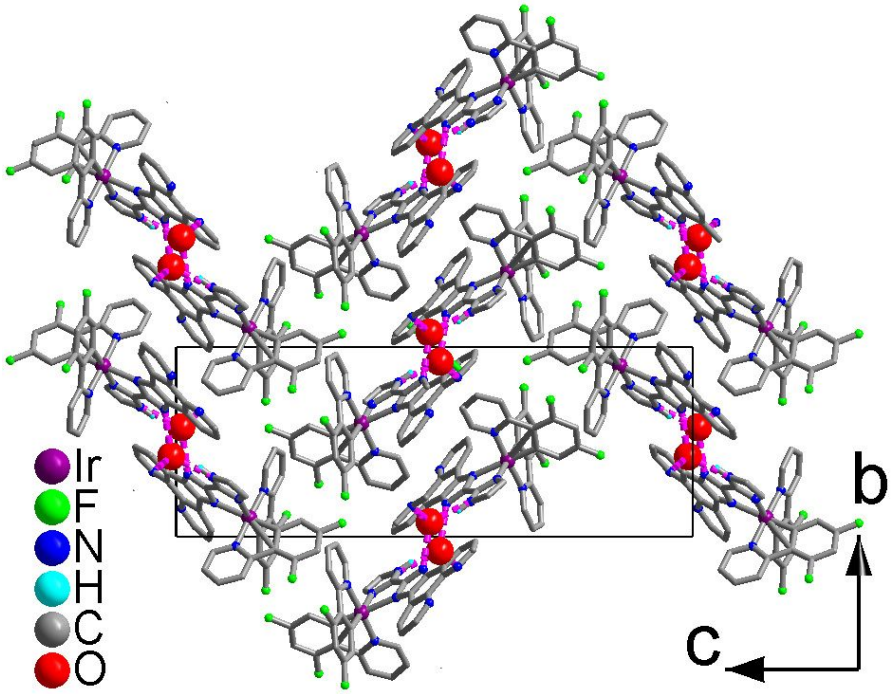

Figure S10 The packing structure of complex **2**·H_2O. Big red balls are O atoms from lattice water molecules.

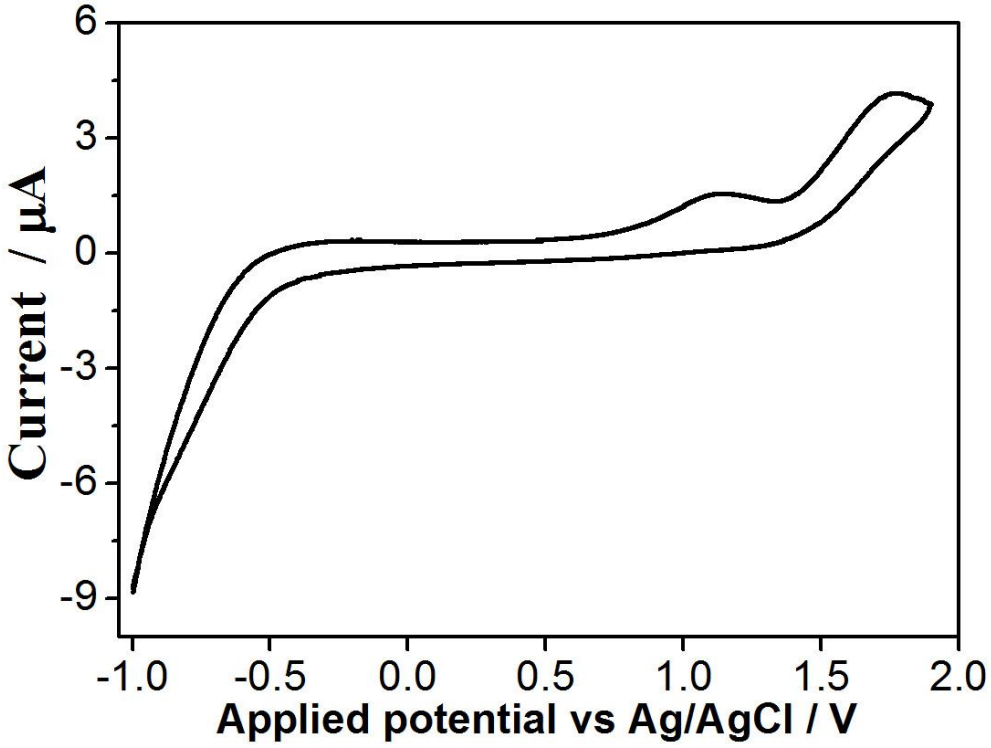

Figure S11 Cyclic voltammogram of imiphenH_2 in DMSO-H_2O mixture (v/v = 50/50) containing 100 mM NaCl and 10 mM PBS (pH = 7.4) with a scan rate 0.1 V/s.

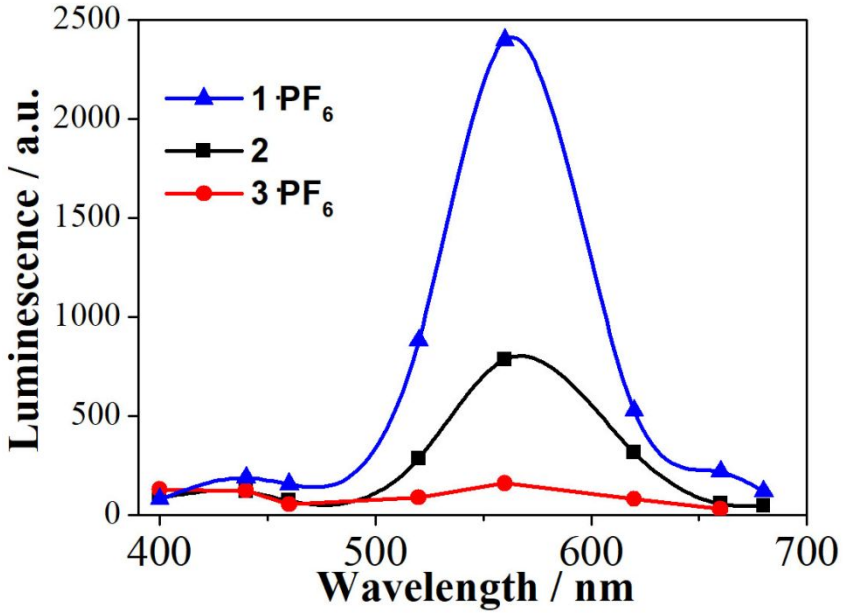

Figure S12. ECL emission spectra of **1**·PF_6, **2** and **3**·PF_6 in DMSO-H_2O mixture (v/v = 50/50) containing 1 mM TPA, 100 mM NaCl and 10 mM PBS (pH = 7.4) at room temperature.

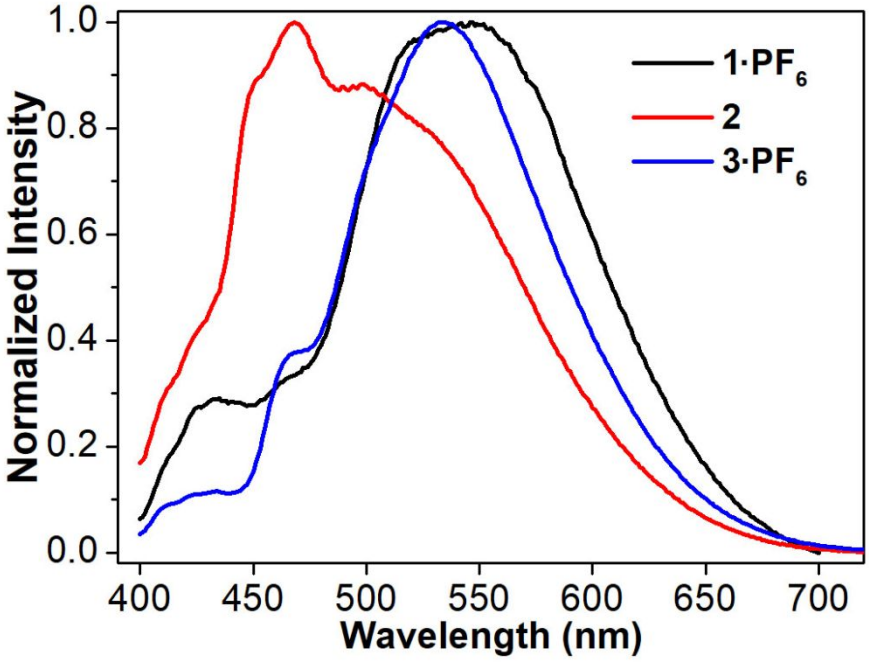

Figure S13. Photoluminescence spectra of **1**·PF_6, **2** and **3**·PF_6 in DMSO-H_2O mixture (v/v = 50/50, c =1×10^{-4} M) at room temperature.

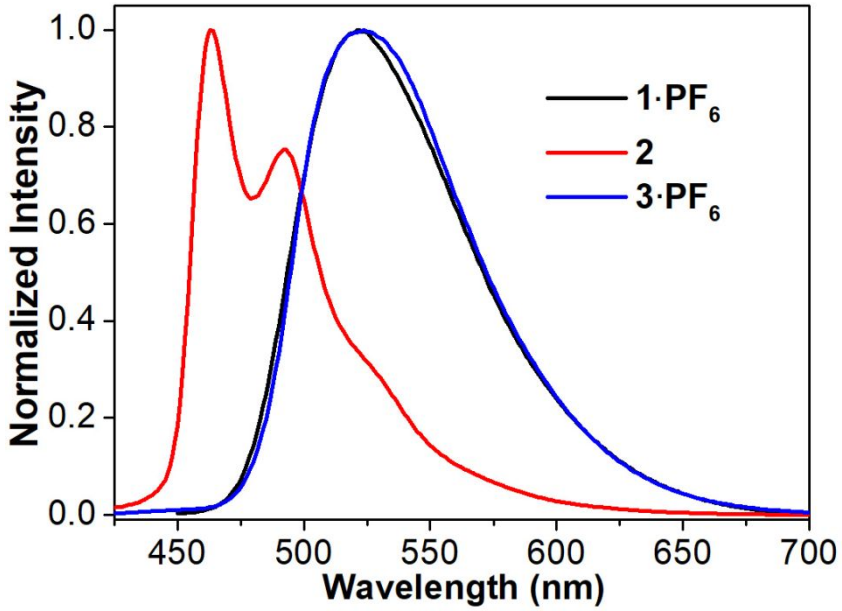

Figure S14. Photoluminescence spectra of **1**·PF_6, **2** and **3**·PF_6 in CH_2Cl_2 (c =1×10^{-4} M) at room temperature [The quantum yields (Φ) were measured in air equilibrated CH_2Cl_2 and determined to be 1.0% for complex **1**·PF_6 (λ_{em}: 521 nm), 9.0% for complex**2** (λ_{em}: 463 and 492 nm), 16.7% for complex **3**·PF_6 (λ_{em}: 524 nm), respectively.].

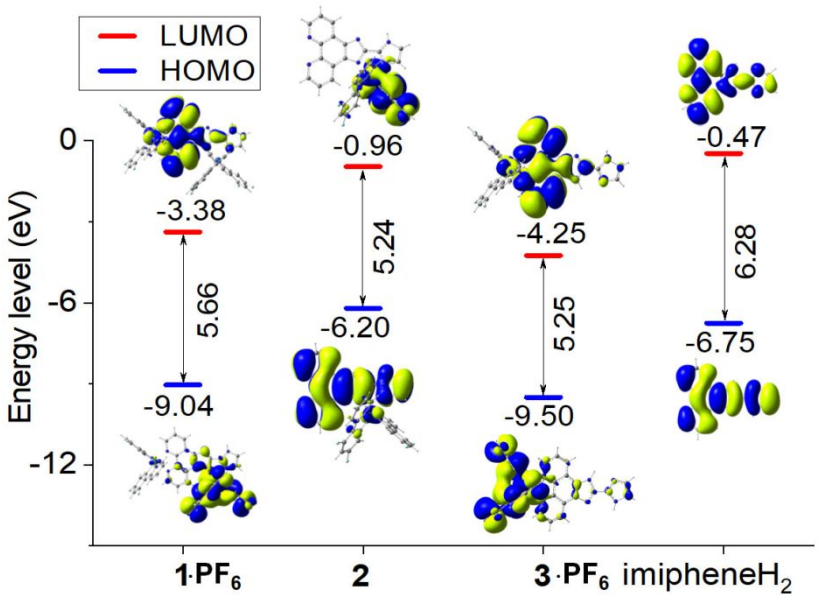

Figure S15. HOMO and LUMO distributions of compounds **1**·PF_6, **2**, **3**·PF_6 and imiphenH_2. The values of frontier molecular orbital energy levels are labeled next to the corresponding symbols. The values of E_{HLG} are also showed directly between the symbols of each compound.

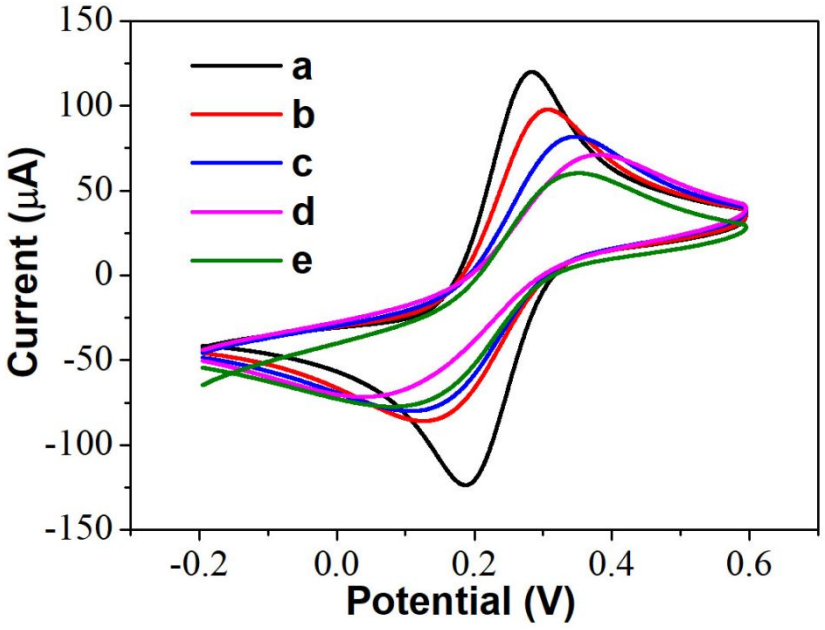

Figure S16. Cyclic voltammetry of (a) bare gold electrode; (b) electrode modified with the capture probe and the blocking molecules (MCH); (c) electrode with the capture probe/MCH/target mi-RNA21; (d) electrode with the capture probe/MCH/target mi-RNA21/auxiliary probes; (e) electrode with the capture probe/MCH/target mi-RNA21/auxiliary probes/complex **1**·PF_6.